

Generating light with a specified spectral power distribution

Ivar Farup, Jan Henrik Wold, Thorstein Seim, and Torkjel Søndrol

A particular version of a spectral integrator has been designed. It consists of a xenon lamp whose light is dispersed into a color spectrum by dispersing prisms. Using a transmissive LCD panel controlled by a computer, certain fractions of the light in different parts of the spectrum are masked out. The remaining transmitted light is integrated and projected onto a translucent diffusing plate. A spectroradiometer that measures the generated light is also attached to the computer, thus making the spectral integrator a closed-loop system. An algorithm for generating the light of a specified spectral power distribution has been developed. The resulting measured spectra differ from the specified ones with relative rms errors in the range of 1%–20% depending on the shape of the spectral power distribution. © 2007 Optical Society of America

OCIS codes: 120.4640, 120.4820, 220.4830, 330.1690.

1. Introduction

In modern color research, the CRT or LCD monitor is frequently used for generating color stimuli. By means of an attached PC unit, a color image of almost any spatial or temporal specification may be displayed on the monitor. The obvious shortcomings, however, are the monitor's limited color gamut and the fact that no metamers can be generated. These deficiencies make the CRT or LCD monitor an inappropriate tool within certain fields of color science and technology, such as color matching and multispectral imaging. What is needed for proper treatment is spectral control, and in this respect the ideal equipment would be an instrument able to generate (within natural limits) the light of a specified intensity and spectral composition. In a work by Hauta-Kasari *et al.*,¹ a spectral synthesizer constructed to synthesize the light corresponding to each filter in a low-dimensional color-filter set is described. The light from a halogen lamp is let through a slit via an optical fiber guide. The resulting collimated beam is made incident on a concave diffraction grating where

the light is reflected and further dispersed onto a transmissive LCD panel placed in the focal plane of the concave grating. By computerized control of the LCD pixels, certain parts of the apparent color spectrum are masked out, and finally the remaining transmitted light is reintegrated by means of a second concave diffraction grating.

Even though the spectral synthesizer has worked as a suitable tool for generating light corresponding to a number of spectrally specified low-dimensional color filters, the considerable light losses implicit in the method used clearly limit the performance of the instrument. For more general uses, high intensities are needed to obtain small spectral bandwidths while still staying above visual thresholds and noise. A construction meeting this latter requirement is an apparatus that uses a high-intensity, high-pressure xenon lamp, comparable to a point source, instead of a halogen lamp, and highly refractive prisms in place of diffraction gratings. By focusing an image of the light source on the instrument's slit aperture, the amount of light let through it is maximized. All the light rays that have passed through the slit are then collected by the remaining optical system. The use of refractive prisms in place of diffraction gratings implies that the light losses associated with higher-order spectra are avoided.

Based on these ideas an updated version of a so-called spectral integrator was built in Basel, Switzerland, in 1968.^{2–4} Four years later an improved version was constructed at the University of Oslo.⁵ Initially, only approximations to light of optimal col-

I. Farup (ivar.farup@hig.no) and T. Søndrol (mail@torkjel.com) are with Gjøvik University College, P.O. Box 191, N-2802 Gjøvik, Norway. J. H. Wold and T. Seim are with the University of Oslo, P.O. Box 1072, Blindern, N-0316 Oslo, Norway.

Received 6 October 2006; accepted 18 December 2006; posted 4 January 2007 (Doc. ID 75814); published 9 April 2007.

0003-6935/07/132411-12\$15.00/0

© 2007 Optical Society of America

ors were generated by the instrument, with wedges moved by digitally controlled stepper motors. These were later replaced by manually cut masks for generating approximations to particular fluorescent light and their corresponding (metameric) blackbody standard reference sources.⁶ However, the time-consuming work of cutting and adjusting the masks, as well as the off-line calibration of the resulting spectra, limited the usefulness of the instrument.

To make more complex experiments feasible, a further upgrade of the spectral integrator has been made.^{7,8} For the masking purpose, a transmissive LCD panel has been placed into the integrator. The panel is controlled by the graphics card of a PC via an analog PAL video interface. For control of the LCD pixels and automation of the spectral recordings, a special software has been developed.^{9,10}

This work aims to give a thorough description of this new upgrade and to show its ability to generate light with a specified spectral power distribution (SPD). The design of the spectral integrator is sketched in Section 2. Section 3 describes the new control software, with particular focus on the calibration algorithm. In Section 4 we present the SPDs of the light generated during calibration and testing of the instrument. The results are discussed in Section 5.

2. Spectral Integrator

A principal sketch of the spectral integrator is shown in Fig. 1. The light source of the integrator is a 2500 W short-arc xenon lamp, which is placed in a specially designed lamphouse H. From the house, two beams of light are tracked along two near-identical optical pathways, the primary branch (solid line) and the secondary branch (dashed line). The primary

branch is described here. By means of a concave mirror M1 placed behind the lamp and an aspherical condenser lens L1 positioned in front of it, a double image of the light source is focused on a water-cooled vertical slit S. (By focusing the mirror image of the light source slightly lower than the primary image, the distribution of light along the slit is optimized. The slit is curved in order for its dispersed image to be straight, which is important for the method used for generating spectral stimuli; see Subsections 3.B and 3.C.) Immediately after the slit, the light is condensed by the condensing lens L2 and thereafter let through a collimator lens L3. The collimated light is then dispersed horizontally through two equilateral prisms, P1 and P2, after which it is let through a circular aperture A. By means of the condensing lens L4, a sharp image of the slit aperture S is focused onto a transmissive LCD panel P placed in the focal plane of this lens. Because of the dispersion, this image forms a full color spectrum. By manipulating the pixels of the LCD panel, one can now control which fractions of the light should be let through the panel in the different parts of the spectrum. Finally, the transmitted components are reintegrated by means of the condensing lens L5, which is positioned so that aperture A is imaged sharply onto a translucent diffusing plate D. Owing to the manipulations of the pixels of the LCD panel, the color of the chromatically homogeneous field now apparent on the diffusing plate will generally be different from the color one would observe on a diffusing plate placed in the plane of aperture A itself. [The function of the two plane mirrors M2 and M3 (front coated) is to reduce the overall size of the instrument.]

As an option, a biprism B may be inserted immediately after the second prism P2 so that two color spectra are projected onto the LCD panel, one placed above the other. By manipulating the LCD pixels in each spectrum region independently, light of two different SPDs is generated. Thus what is seen on diffusing plate D is a bipartite field, i.e., an image of the biprism centered within aperture A, one half of which is of a color corresponding to one light and the other half is of a color corresponding to the other light. By letting the LCD pixels be manipulated by, e.g., a PC mouse, typical color-matching experiments can now be performed. Using the secondary branch of the spectral integrator to generate a field that surrounds the bipartite field, it will also be possible to perform color-matching experiments under various adaptation conditions.

A vital part of the instrumental setup is the spectroradiometer (Minolta CS-1000) R that is integrated with the optical system through an administrative PC. Being managed by a computer, the spectroradiometer measures the variety of generated light automatically, without any manual reading or mechanical manipulation. Moreover, all the measured data, including the SPDs, are saved in files for further treatment and/or computation. As a result of the integrated design, the precision achieved both in the generation of light and in the measurement of the spectroradiometric data is significantly improved relative to the precision ob-

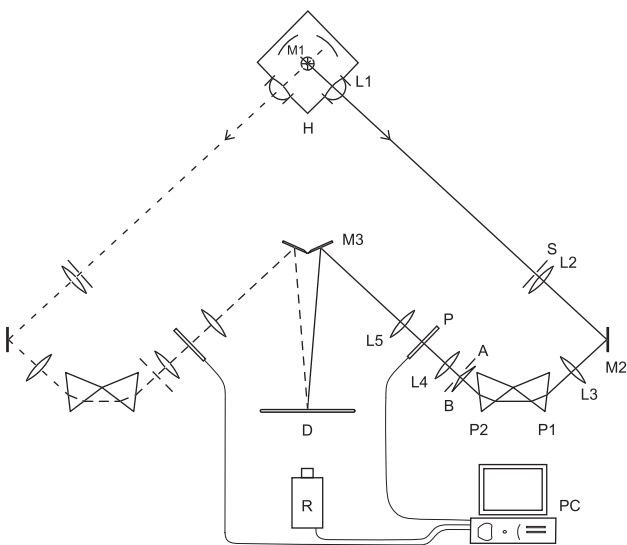


Fig. 1. Principal sketch of the spectral integrator: H, lamphouse; M1, concave mirror; L1, aspherical condenser lens; S, water-cooled vertical slit; L2, condensing lens; M2, plane mirror; L3, collimator lens; P1 and P2, equilateral dispersing prisms; B, (optional) biprism; A, circular aperture; L4, condensing lens; P, transmissive LCD panel; L5, condensing lens; M3, plane mirror; D, translucent diffusing plate; R, spectroradiometer; PC, administrative PC.

tained by means of the former, manually controlled integrator.^{5,7,8}

3. Controlling the Spectral Integrator

A. Software Architecture

The control software for the spectral integrator has been developed in Microsoft Visual Studio .NET using Visual C++ as the development language.⁹ This gives the flexibility necessary to create a graphical user interface (GUI), as well as to communicate through the serial port with external devices such as the LCD panel and the spectroradiometer. It also provides the computational speed needed for generating light with a specified SPD (see Subsections 3.B and 3.C).

To create a flexible and extendable software, the program is designed as a kernel with supporting modules. The kernel is a stand-alone Windows application, whereas the modules are implemented as Dynamic Link Library (DLL) files that are loaded at start-up. The kernel is responsible for the overall GUI as well as for facilitating communication between the modules. The modules are responsible for different subtasks, and each module provides its own GUI.

The responsibilities of the different modules are as follows:

- The spectral integrator module is responsible for drawing the mask on the LCD panel. This can be achieved in two ways: Pixels can be opened individually, or a SPD can be specified. In the latter case, data from the calibration module (see below) are used in conjunction with the algorithm presented in Subsection 3.C.
- The spectroradiometer module communicates with the spectroradiometer through the serial port. The spectroradiometer is configured, measurements requested, and results communicated.
- The input device module is in charge of communicating with the external input device (e.g., a PC mouse) used in color-matching experiments (see color-matching module).
- The calibration module communicates with both the spectroradiometer module and the spectral integrator module. It signals the spectral integrator module to open certain LCD pixels and then signals the spectroradiometer module to measure the SPD of the resulting light. In this way, all the data needed for construction of the model presented in Subsection 3.B are obtained.
- The color-matching module is used to perform color-matching experiments. One test stimulus and three reference stimuli can be generated simultaneously. The test stimulus is presented in one half of a bipartite field (the test field) and the reference stimuli in the other half (the reference field). By means of the input device module, the observer can adjust the intensity of each reference stimulus independently to obtain a color match (in the sense that the two halves appear as one homogeneously colored field). If a color match cannot be achieved this way, the observer is

allowed instead to mix the stimulus represented in the test field with one or more of the reference stimuli, thereby trying to obtain a match.

- The primary generator module is used to generate light with Gaussian shaped SPDs, which are used as reference stimuli in color-matching experiments.
- The script parser module is used when sequential experiments are to be performed. The module can be used both for generating and executing scripts that utilize the functionality supplied by the kernel and the other modules.

B. Characterization of the Spectral Integrator

The location of the color spectrum on the LCD panel is determined automatically by means of a binary search algorithm. Initially, all the pixels are closed, and the total energy is measured and recorded. Then one half of the panel is opened. If the result of this is that the measured energy changes significantly, we assume that at least some part of the color spectrum is inside the opened area. In this manner, we continue halving and measuring the opened part recursively until one edge of the color spectrum is found. The same procedure is applied for the other three edges. In this way, a window M pixels high and N pixels wide is localized. (Typical values for the present configuration of the spectral integrator are $M \sim 100$ and $N \sim 200$.) In the following, this window is referred to as the color spectrum window.

To check that the LCD panel is sufficiently well aligned with the color spectrum, the top and the bottom halves of the central vertical line of the color spectrum window are opened successively and the respective SPDs (alignment functions) measured.

The main factor limiting the spectral resolution is the width of the (1 mm) slit S in Fig. 1. For a monochromatic light source, the width of the slit image on the LCD panel is approximately 0.5 mm in the red region, i.e., a width of approximately 2 LCD pixels, corresponding to approximately 4 pixels on the monitor of the administrative PC. To get better control and achieve reasonable intensities when generating light of specified SPDs, the lines on the PC monitor are normally chosen to be 2 pixels wide. For similar reasons, a linewidth of 2 pixels is used for the creation of horizontal lines. By using 2×2 pixel blocks on the PC monitor, also the computational complexity is reduced. Since the use of blocks instead of single pixels does not affect the way the algorithms below are constructed, we will continue to refer to pixels, although each such may actually be a pixel block. Thus what is referred to as a line on the LCD panel will in fact correspond to a line of pixel blocks on the PC monitor.

For the calibration routine, the following definitions apply:

- Black spectrum: the SPD of the light remaining when all the pixels of the LCD panel are closed.
- Global white spectrum: the SPD of the light generated when all the pixels of the color spectrum window are opened.

- Local white spectrum: the SPD of the light generated when a single horizontal line of the color spectrum window is opened (giving a total of M local white spectra).
- Corrected local white spectrum: the SPD corresponding to the difference between the local white spectrum and the black spectrum.
- Aperture function: the SPD of the light generated when a single vertical line of the color spectrum window is opened (giving a total of N aperture functions).
- Corrected aperture function: the SPD corresponding to the difference between the aperture function and the black spectrum.
- Alignment function: the SPD of the light generated when the top or the bottom half of the central vertical line of the color spectrum window is opened (see above).

In the calibration algorithm, a complete characterization of the spectral integrator is achieved by measuring all the local white spectra and aperture functions, in addition to the black spectrum, the global white spectrum, and the two alignment functions. Hence the total number of SPDs to be measured counts $M + N + 4$.

A SPD is by nature a continuous function of wavelength, e.g., $s(\lambda)$. For practical purposes, however, the light's spectral intensity is sampled at chosen wavelengths, implying that the SPD can be represented by a vector, which we, for simplicity, will not distinguish from the SPD itself. Thus denoting by L the number of samples, the black spectrum is represented by an $L \times 1$ column vector \mathbf{b} (since the spectroradiometer used samples the spectrum at every nanometer from 380 to 700 nm, $L = 321$). Similarly, the aperture functions are represented by column vectors $\mathbf{a}_j, j = 1, \dots, N$. The corrected aperture functions are then determined by the equation

$$\bar{\mathbf{a}}_j = \mathbf{a}_j - \mathbf{b}, \quad (1)$$

whose resulting vectors are subsequently arranged in an $L \times N$ matrix

$$\mathbf{A} = [\bar{\mathbf{a}}_1 \dots \bar{\mathbf{a}}_N]. \quad (2)$$

The use of 2×2 pixel blocks ensures that the intensity of the light described by each aperture function becomes sufficiently high for precise measurements.

The reason for measuring the local white spectra is that the color spectrum is not homogeneously distributed vertically over the LCD panel. For each horizontal line opened, a local white spectrum $\mathbf{v}_i, i = 1, \dots, M$, similar to (but with proportionally lower intensity values than) the global white spectrum is measured. The corresponding corrected local white spectra are then given as

$$\bar{\mathbf{v}}_i = \mathbf{v}_i - \mathbf{b}. \quad (3)$$

From these spectra, the weighting factors for estimating the specified SPDs from the corrected aperture functions can be determined. We are, however, not interested in the weight as a function of wavelength, but as a function of pixel position. This latter is obtained by first determining the indices of the maximum elements of $\bar{\mathbf{a}}_j, j = 1, \dots, N$, i.e.,

$$k_j = \arg \max(\bar{\mathbf{a}}_j), \quad (4)$$

and then arranging the corresponding corrected local white spectra into an $M \times N$ weighting matrix \mathbf{W} whose element W_{ij} is given by the k_j th element of $\bar{\mathbf{v}}_i$:

$$W_{ij} = (\bar{\mathbf{v}}_i)_{k_j}. \quad (5)$$

Finally, the weighting matrix is normalized according to

$$\bar{W}_{ij} = \frac{W_{ij}}{\sum_i W_{ij}}, \quad (6)$$

such that $\sum_i \bar{W}_{ij} = 1$. The normalized element \bar{W}_{ij} then yields the contribution from the pixel with index ij to the corrected aperture function $\bar{\mathbf{a}}_j$, and the SPD, \mathbf{s}_{ij} , of the light generated by opening this pixel is thus (according to the criteria above) given as

$$\mathbf{s}_{ij} = \bar{W}_{ij} \bar{\mathbf{a}}_j + \mathbf{b} \quad (7)$$

(the black spectrum \mathbf{b} being subtracted from each aperture function and added once for the resulting spectrum).

C. Algorithm for Generating Light with a Specified Spectral Power Distribution

When light of a specified SPD is to be generated, the crucial task is to create an appropriate mask in the color spectrum window localized by the binary search algorithm described in Subsection 3.B. To reduce the possible effects of pixel boundaries, and in an attempt to make the color field appearing on the diffusing plate D in Fig. 1 as homogeneous as possible, this is done by starting from the central horizontal line of the window and successively opening neighboring pixels symmetrically above and below this line (see the rightmost diagrams in Fig. 3 below). The LCD panel mask (the subset of all the pixels) thus obtained can be described by an $N \times 1$ integer vector \mathbf{m} , whose element $m_j \in \{0, 1, \dots, M\}$ is the number of pixels opened at the j th vertical line of the color spectrum window. The weights of the various aperture functions are then given by the $N \times 1$ vector \mathbf{w}_m whose elements are obtained by summing the weights of the opened pixels, i.e.,

$$(\mathbf{w}_m)_j = \sum_{i=\lfloor (M-m_j)/2 \rfloor}^{\lfloor (M-m_j)/2 \rfloor + m_j} \bar{W}_{ij}, \quad (8)$$

where $\lfloor \dots \rfloor$ denotes the mathematical floor. For a given LCD panel mask described by \mathbf{m} , the estimated SPD of the resulting light \mathbf{s} is now given as

$$\mathbf{s} = \mathbf{Aw}_m + \mathbf{b}. \quad (9)$$

Equation (9) summarizes what may be called the forward model, i.e., the method for estimating the SPD of light generated by means of a LCD panel mask specified by vector \mathbf{m} . What is of major interest, however, is the reverse procedure, i.e., to specify a SPD \mathbf{s}' and find the vector \mathbf{m} that yields a SPD as close to this as possible. This can be done, e.g., by minimizing

$$\|\mathbf{s}' - \mathbf{s}\| = \|\mathbf{s}' - (\mathbf{Aw}_m + \mathbf{b})\| \quad (10)$$

with respect to \mathbf{m} . This is a standard nonlinear constrained N -dimensional combinatorial optimization problem, and several algorithms for solving it are known.¹¹ However, such algorithms are generally quite time consuming and do not exploit *a priori* information. For color-matching experiments, it is of utmost importance that LCD panel masks can be generated in real time, which requires that a mask be generated within 40 ms (corresponding to generating 25 frames/s). To meet this requirement, a heuristic search algorithm has been developed:

1. Initiate by setting $l = 1$ and $\mathbf{m}_l = \mathbf{0}$.
2. From the current estimate \mathbf{m}_l , compute the estimated SPD, \mathbf{s}_l , using Eq. (9), i.e., $\mathbf{s}_l = \mathbf{Aw}_{m_l} + \mathbf{b}$.
3. Compute the difference vector, $\mathbf{d}_l = \mathbf{s}' - \mathbf{s}_l$, where \mathbf{s}' is the specified SPD to be approximated (the target spectrum).
4. For every element $(\mathbf{d}_l)_k$ of \mathbf{d}_l , find the index j for which $|k - \arg \max(\bar{\mathbf{a}}_j)|$ is minimum. Construct the $N \times 1$ vector $\Delta\mathbf{m}_l$ with elements given as $(\Delta\mathbf{m}_l)_k = (\mathbf{d}_l)_k / (\sum_i (\bar{\mathbf{a}}_j)_i / M)$. (Assuming that the weight of each pixel is $1/M$ instead of \bar{W}_{ij} in order to improve the speed of the algorithm, the total energy contribution by one pixel at line j is $\sum_i (\bar{\mathbf{a}}_j)_i / M$. Thus the elements of the vector $\Delta\mathbf{m}_l$ correspond to the number of pixels that need to be opened or closed to increase or decrease the intensity of the light described by the respective aperture functions sufficiently.)
5. Round the elements of $\Delta\mathbf{m}_l$ in a manner inspired by error diffusion algorithms for half-toning.¹² Start by rounding the first element toward the nearest integer, and then add the round-off error to the neighboring element. To further reduce systematic errors, perform the error diffusion alternately forward and backward through the vector $\Delta\mathbf{m}_l$. Denote the vector rounded in this manner $\bar{\mathbf{m}}_l$. (The elements of $\Delta\mathbf{m}_l$ are real numbers, whereas the numbers of pixels to be opened or closed must be integers. Experiments have shown that a simple round off of the real numbers can lead to quite large systematic errors and cause the iterative algorithm to stop prematurely.)
6. Update the estimates of the elements of \mathbf{m} according to $(\mathbf{m}_{l+1})_j = \min(\max((\mathbf{m}_l)_j + (\Delta\bar{\mathbf{m}}_l)_j, 0), M)$.
7. If $\mathbf{m}_{l+1} \neq \mathbf{m}_l$, increase l by one and iterate from step 2, otherwise accept $\mathbf{m} = \mathbf{m}_{l+1}$ as the best estimate for the LCD panel mask.

The algorithm works in real time. For smoothly curved SPDs, the number of iterations is typically

five, whereas, for piecewise linear SPDs, the number of iterations can approach 20.

However, since the algorithm above is based on Eq. (9), which in turn involves simplifying approximations, the resulting generated light is not exactly equal to the one specified. To improve the performance, an additional iterative algorithm has been implemented. Instead of using the forward model summarized in Eq. (9), the LCD panel mask configuration and the spectroradiometer measurements are here included in the computations, thereby making a true closed-loop system. At the cost of prolonging the time needed to generate a specific light from a few milliseconds to a few minutes, an even better approximation to the specified SPD is now obtained. Using this algorithm in combination with the former solely numerically based method has proved particularly efficient. Initially, a preliminary estimate of vector \mathbf{m} representing the LCD panel mask is obtained using the algorithm described in steps 1–7 above. Then an improved result is obtained by means of the additional algorithm, whose directives are identical to those of the former, except for the first step, which is dropped, and the second step, which is replaced by the following:

- 2'. Draw the mask represented by \mathbf{m}_l on the LCD panel and let \mathbf{s}_l be the measured SPD of the light generated.

Vector \mathbf{m} determined in this way can be saved for future use and will remain valid as long as the spectral integrator does not need recalibration.

4. System Performance

A. Calibration

Black spectrum \mathbf{b} is shown separately in Fig. 2(a). In Fig. 2(b) the black spectrum (dashed curve) and the global white spectrum (solid curve) are plotted in the same diagram, thus indicating the range of light that is possible to generate by means of the spectral integrator. As seen, the global white spectrum shows rather low values in the short-wavelength region. This is partly attributable to absorption of high-frequency light in the two prisms made of dense flint glass, but the main reason is the properties of the LCD panel used (see Subsection 5.B). Furthermore, the global white spectrum shows pronounced spikes in the long-wavelength region owing to the physical properties of the xenon gas in the short-arc lamp.

The corrected aperture functions $\bar{\mathbf{a}}_j, j = 1, \dots, N$, are shown in Fig. 2(c). One should note that the aperture functions are narrower and more closely spaced toward the violet part of the color spectrum. This is because the refraction of light in the prisms is strongest for the shorter wavelengths. As a consequence, it is possible to generate more accurate SPDs in the short- than in the long-wavelength region of the spectrum. It can also be observed that some of the aperture functions in the long-wavelength region are not very smooth and even show some of the spikes that are also apparent in the white spectra.

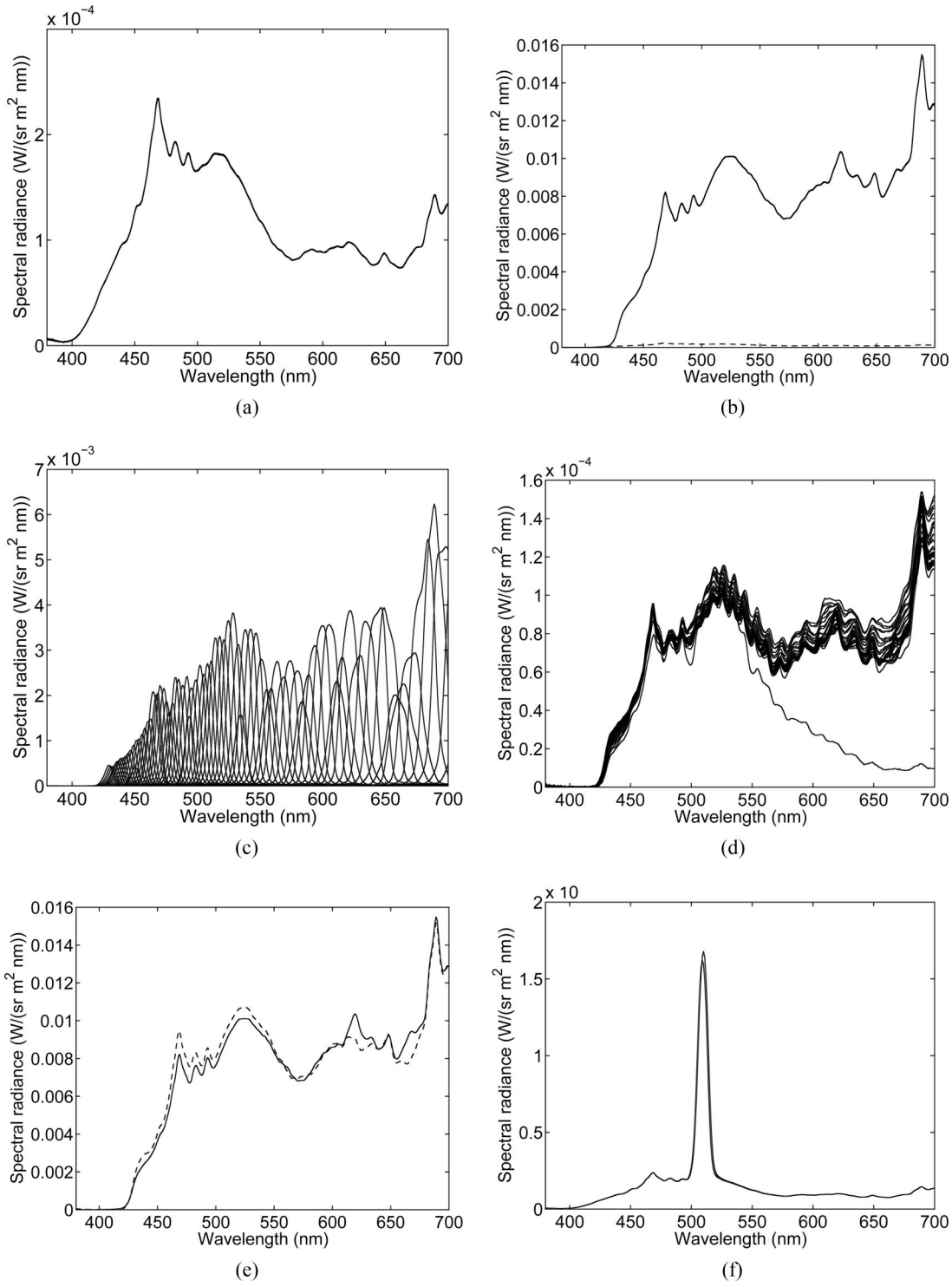


Fig. 2. Spectral properties of the spectral integrator. (a) Black spectrum, (b) global white spectrum (solid) and black spectrum (dashed), (c) aperture functions for each of the vertical lines, (d) local white spectra for each of the horizontal lines, (e) global white spectrum (solid) and sum of aperture functions (dashed), and (f) alignment functions (see Subsection 4.A).

The measured local white spectra \mathbf{v}_i , $i = 1, \dots, M$, are shown in Fig. 2(d). The diagram shows that there is some variation vertically across the LCD panel. One of the local white spectra, the one corresponding to the lowermost pixel line of the color spectrum window, differs quite drastically from the other ones

in having attenuated values in the long-wavelength region. This results from a nonperfect alignment of the LCD panel with the dispersing prisms, implying that the edges of the color spectrum are not exactly parallel with the pixel lines of the LCD panel. Consequently, parts of the border lines of the color spec-

trum window can drop outside the color spectrum itself. However, this problem is taken care of by the calibration procedure.

A fundamental assumption of the model presented in Subsection 3.B is that the spectral integrator operates linearly in the sense that the SPD of the light generated by opening two vertical lines on the LCD panel equals the sum of the SPDs describing the light obtained when the same lines are opened one at a time. This hypothesis can be tested by summing all the aperture functions. If the assumption is correct, the global white spectrum shown in Fig. 2(b) should be obtained. The sum of the aperture functions is shown in Fig. 2(e) (dashed curve) along with the actual global white spectrum (solid curve). As seen, the two spectra are similar, although not exactly equal (see Subsection 5.A). In particular, one observes that in the long-wavelength region, the global white spectrum is considerably more spiky than expected from the sum of the aperture functions. This is partly because the SPD of the xenon light source has considerably more spikes in this region and partly because

the lower refractive indices for the longer wavelengths increase the bandwidths of the aperture functions and thus reduce the possibility of controlling the resulting SPD.

The two alignment functions are shown in Fig. 2(f). Their peaks are 1 nm apart, indicating that the panel is fairly well aligned with the color spectrum. The slight misalignment still present contributes to making the aperture functions slightly wider than optimally achievable.

B. Generation of Light with a Specified Spectral Power Distribution

Using the calibration data from Subsection 4.A and the algorithm given in Section 3, approximations to light of different specified SPDs can now be generated. Figure 3 shows the SPDs and the LCD panel masks involved in the generation of light that closely corresponds to a magenta optimal color. Figure 3(a) shows the specified optimal color (dotted lines) plotted together with the SPD calculated by running the

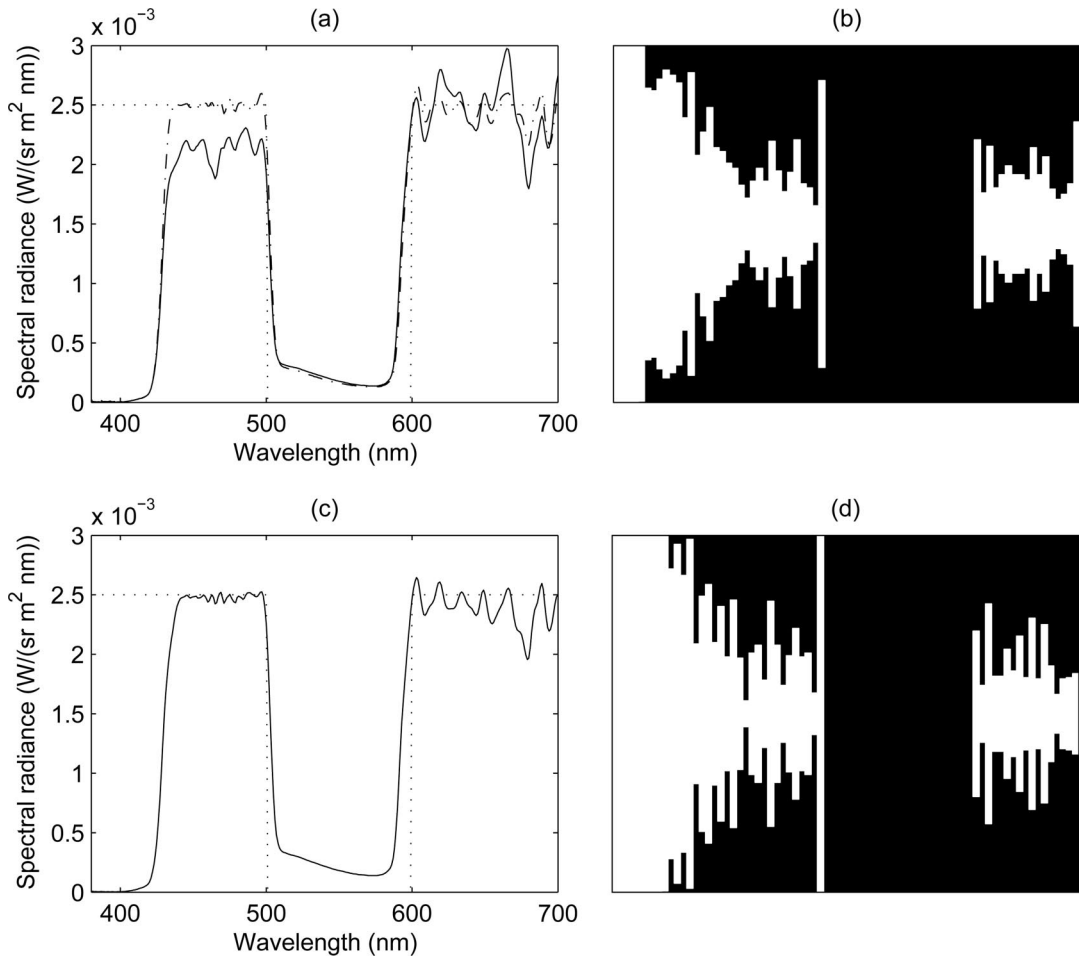


Fig. 3. Generation of light corresponding to a magenta optimal color. (a) The specified optimal color (dotted), the SPD calculated by running the algorithm given in steps 1–7 in Subsection 3.C (dash-dotted), and the corresponding SPD measured by the spectroradiometer (solid); (b) the numerically determined LCD panel mask; (c) the specified optimal color (dotted) and the SPD of the corresponding approximated light resulting from including the spectral integrator and the spectroradiometer in the optimization loop (solid); and (d) the final optimized LCD panel mask (see Subsection 4.B).

dotted curve) and the SPD measured by the spectroradiometer (solid curve). The corresponding LCD panel mask is shown in Fig. 3(b). As one would expect, the measured SPD shows too low values in the short-wavelength region and a too spiky curvature in the long-wavelength region.

In Fig. 3(c) the SPD of the light resulting from including the spectral integrator and the spectroradiometer in the optimization loop (solid curve) is shown together with the specified optimal color (dotted lines). The corresponding LCD panel mask is shown in Fig. 3(d). After this latter iteration, the

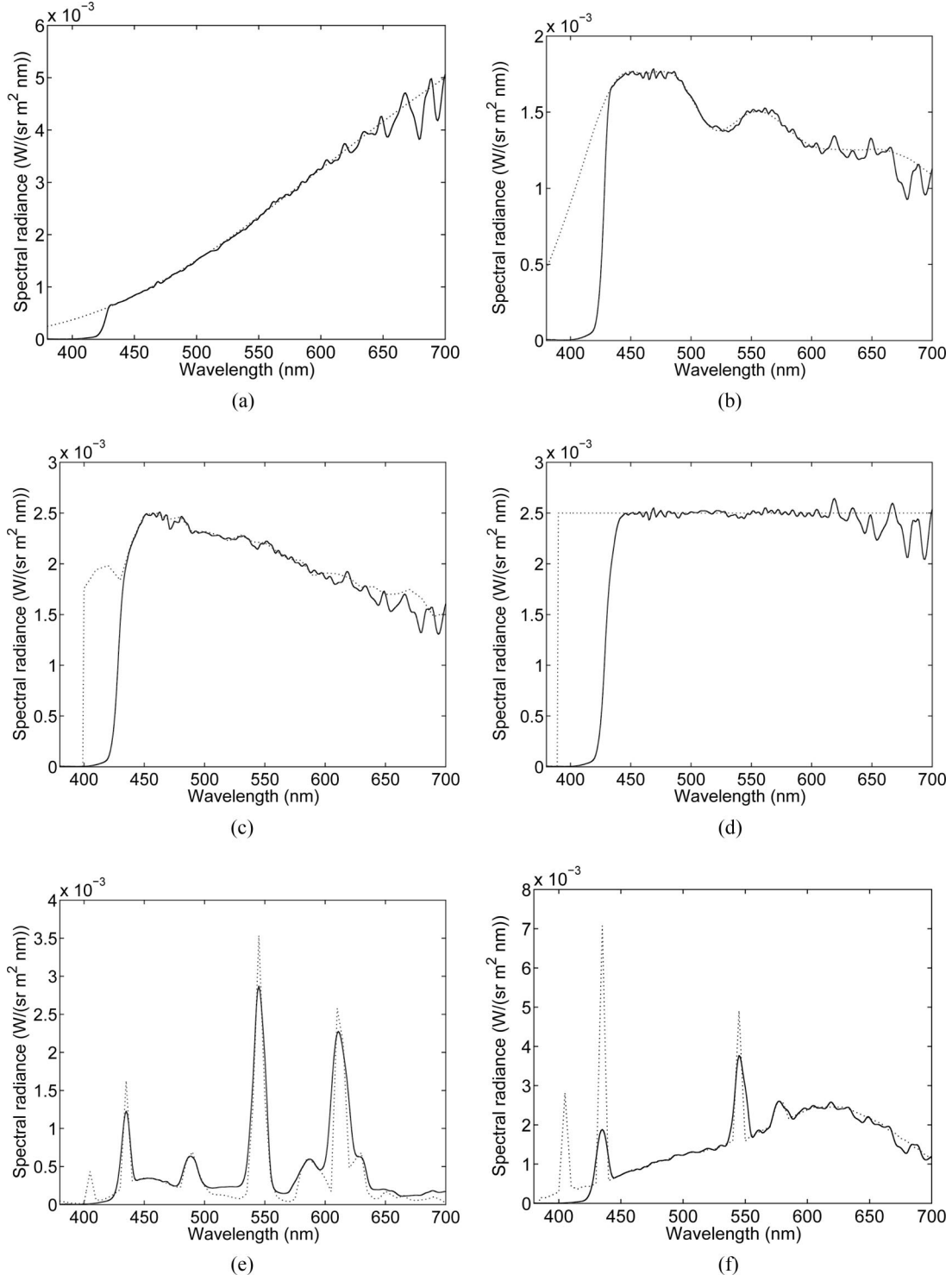


Fig. 4. Standard illuminants and SPDs of commercial light sources, as specified (dotted) and as generated (solid). (a) Illuminant A, (b) illuminant C, (c) illuminant D65, (d) illuminant E, (e) SPD of TL84, and (f) SPD of Cool White Deluxe.

deviations are significantly reduced, and the spikes attenuated. As is apparent from Fig. 3 the reduction of spikes in the SPD is achieved by introducing more pronounced spikes in the LCD panel mask. However,

it appears to be impossible to avoid the spikes completely with the present method. Finally, it should be noted that the spectral intensities in the medium-wavelength regions in Figs. 3(a) and 3(c) deviate

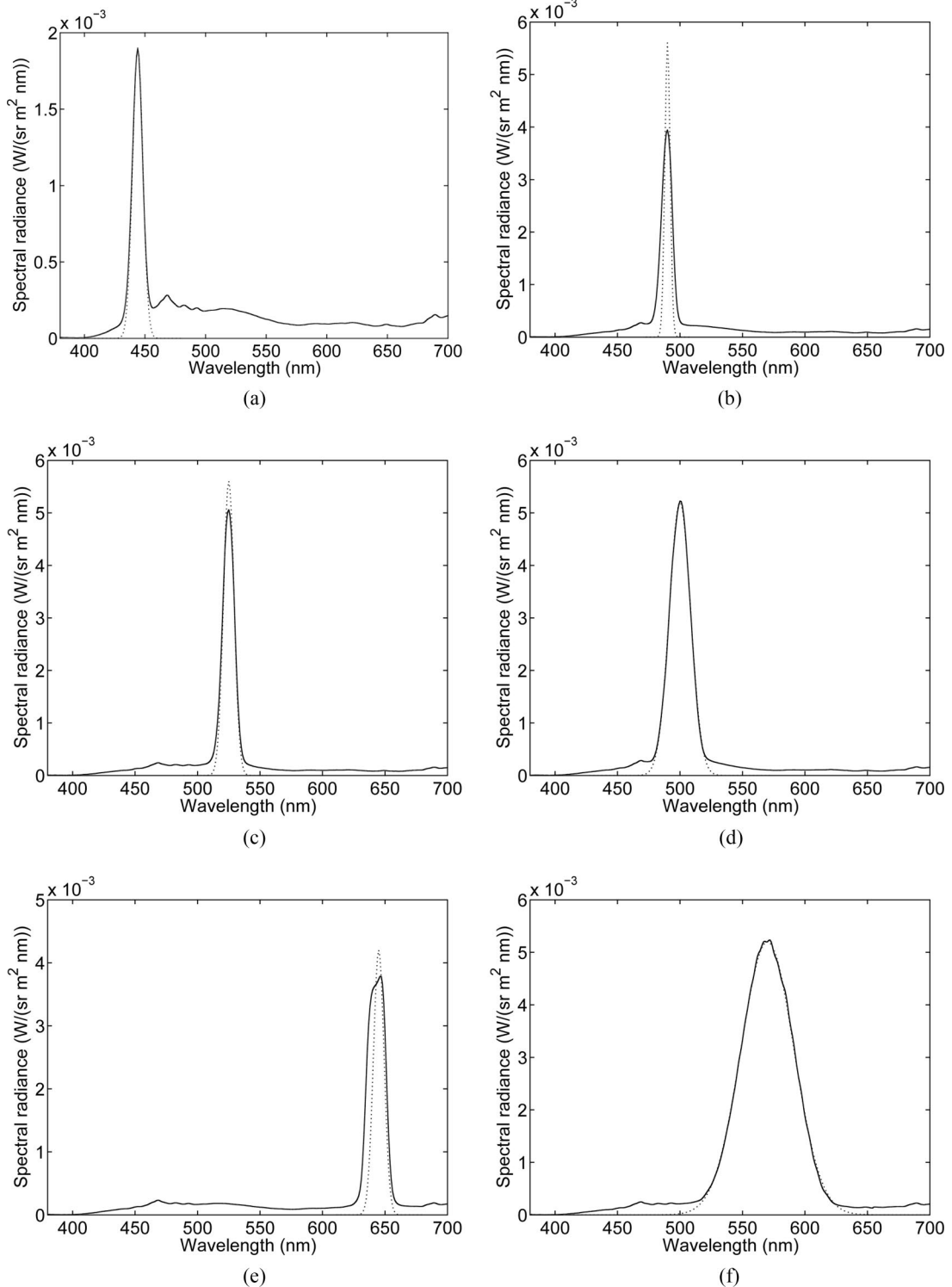


Fig. 5. SPDs of the Stiles RGB reference stimuli (left) and other Gaussian shaped SPDs (right), as specified (dotted) and as generated (solid). (a) Stiles reference stimulus B, centered at 444.4 nm with a bandwidth of 10 nm; (c) Stiles reference stimulus G, centered at 525.3 nm with a bandwidth of 10 nm; (e) Stiles reference stimulus R, centered at 645.2 nm with a bandwidth of 10 nm; (b) Gaussian shaped SPD centered at 490 nm with a bandwidth of 5 nm; (d) Gaussian shaped SPD centered at 500 nm with a bandwidth of 20 nm; and (f) Gaussian shaped SPD centered at 570 nm with a bandwidth of 50 nm.

markedly from zero. This is mainly because of insufficient attenuation of light when the LCD pixels are closed.

C. Generation of Particular Spectral Light

The performance of the spectral integrator has been tested by generating approximations to light with different types of SPD: standard illuminants, SPDs of commercial fluorescent light sources, smooth narrowband SPDs, multimodal SPDs, and particular optimal colors.

In Figs. 4(a)–4(d) illuminants A, C, D65, and E (dotted curves) are plotted together with the measured SPDs of the respective approximations generated (solid curves). The general trend is clear: The SPDs are reproduced quite nicely, except for the cutoff in the short-wavelength region and the spikes in the long-wavelength region, none of which can be compensated for by the LCD panel mask. The results suggest that the generation of light with smooth SPDs is in some sense less challenging than the generation of light whose SPDs have straight line segments. This is not surprising since the graphs of the aperture functions are themselves smoothly curved.

Figures 4(e) and 4(f) show the measured SPDs of two commercial fluorescent light sources, TL84 and Cool White Deluxe (dotted curves), along with the measured SPDs of the respective generated approximations (solid curves). [TL84 is a narrow-triband fluorescent lamp with correlated color temperature of 4000 K and a SPD similar to the Commission Internationale de l'Eclairage (CIE) Illuminant F11, and Cool White Deluxe is a broadband fluorescent lamp with correlated color temperature of 4150 K and a SPD similar to the CIE Illuminant F9.] Similar deviations are seen as for the standard illuminants, but, in addition, the diagram indicates that the spectral integrator has some problems reproducing very narrow spikes. Obviously, the most narrow spikes achievable are the aperture functions themselves

[Fig. 2(c)]. Because of the cutoff below approximately 425 nm, the spikes in the short-wavelength region of the TL84 and Cool White Deluxe SPDs are attenuated or lost.

For the purpose of performing color-matching experiments, the spectral integrator is able to generate test stimuli with narrow Gaussian shaped SPDs, solely from specifications of dominant wavelength, bandwidth, and intensity. Figures 5(a), 5(c), and 5(e) show the SPDs of the Stiles RGB reference stimuli^{13,14} (dotted curves) together with the measured SPD of the respective reconstructions generated by the spectral integrator (solid curves). Figures 5(b), 5(d), and 5(f) display some freely chosen Gaussian shaped SPDs (dotted curves), each along with the measured SPD of the approximation generated (solid curves). The results are quite satisfactory as long as the specified bandwidths are not too narrow. However, owing to insufficient attenuation of light in the closed LCD pixels, the colorimetric purities of the generated stimuli are not optimal.

In color-matching experiments, one will normally need to combine reference stimuli of Gaussian shaped SPDs in order to obtain a color match. Hence the SPD of the resulting stimulus will be either bimodal or trimodal. An example of a best fit (solid curve) to a specified bimodal SPD (dotted curve) is shown in Fig. 6(a).

To test the spectral integrator's capability to generate light with a piecewise linear SPD, a few syntheses of light were made using optimal colors as target spectra. Figures 3(c) and 6(b) show the resulting measured SPD (solid curve) when the target spectrum (dotted lines) is a magenta and a green optimal color, respectively. Also in these cases, the results are quite satisfactory. Approximations to light closely corresponding to blue and red optimal colors have also been generated, but since their SPDs are almost equal to the left- and the right-hand sides, respectively, of the SPD shown in Fig. 3(c), separate plots are omitted.

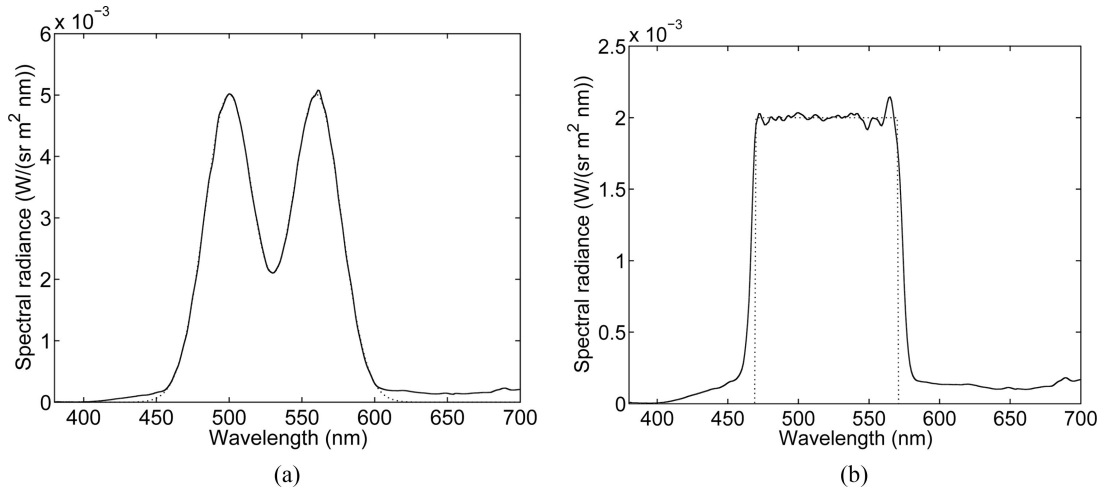


Fig. 6. Bimodal SPD and a green optimal color as specified (dotted) and as measured for the corresponding approximated light generated by the spectral integrator (solid). (a) Bimodal SPD of light synthesized from two components with Gaussian shaped SPDs, and (b) green optimal color.

5. Discussion

A. Spectral Accuracy of the Generated Light

The relative spectral rms error of a SPD is defined as follows:

$$e_{\text{rms,rel}} = \frac{\sqrt{\sum_{i=1}^L (s_i' - s_i)^2}}{\sqrt{\sum_{i=1}^L s_i'^2}}, \quad (11)$$

where s_i' and s_i are the spectral components of the specified and the measured SPD, respectively. The computed relative spectral rms error for each generated light is given in Table 1. The difference between the calculated closest estimate and the measured spectrum results mainly from the assumptions made for the forward model leading to Eq. (9), whereas the difference between the specified SPD and its calculated closest estimate stems partly from the algorithm presented in Subsection 3.C and partly from the physical limitations inherent to the equipment itself.

As is apparent from Fig. 2(e), the sum of the aperture functions is similar to the global white spectrum, although not exactly equal. In the short-wavelength region, the sum of the aperture functions is smaller than expected, whereas toward the longer wavelengths, the sum is greater. This may be the result of several effects. First, the signal received by the LCD panel has been converted to an analog PAL signal for transmission. Thus the edges from black to white are smeared out somewhat. This edge effect is obviously

more prominent for narrow lines (as for the aperture functions) than for continuous open areas (as for the global white spectrum). For future improvements of the spectral integrator, a digital transmission from the administrative PC to the LCD panel should be considered. Second, the aperture functions are narrower and overlap more in the short-wavelength region, which implies that the algorithm presented in Subsection 3.C will tend to generate a SPD with too low intensity values in the short-wavelength region and too high intensity values in the long-wavelength region.

B. Loss of Light in the Optical System

The narrow width of the slit S is the main reason for the loss of light in the optical system. However, this does not account for the particular loss of light observed in the short-wavelength region up to approximately 425 nm [see Fig. 2(b)]. The optical component predominantly responsible for this is the LCD panel, which attenuates the light significantly at all wavelengths, but particularly heavily below 425 nm. In addition to the LCD panel the dense flint glass of the two prisms also contributes somewhat to the light in the short-wavelength region. The many lenses and front-coated mirrors in the optical pathway only slightly reduce the spectral power at short wavelengths.

C. Future Improvement of the Optical System

The contrast ratio of the LCD panel used is not optimal. A better panel should be used to attenuate the unwanted stray light clearly seen in the shoulders of the alignment functions shown in Fig. 2(f). The LCD panel can also be replaced by a digital light processing (DLP) micromirror chip. This will increase the power throughput of the system markedly. Direct digital control of pixels should be implemented in place of the PAL converter used in the present setup.

The dense flint-glass prisms can be replaced by high refractive prisms of other materials that transmit more of the light from the short-wavelength part of the spectrum.

6. Conclusion

During the past decades, a spectral integrator has been built and refined. The apparatus has now been extended with a control software that through a fast iterative algorithm makes the generation of light with a specified SPD with good precision feasible. When the spectroradiometer is included in the iterative loop, a considerable improvement in the match between the SPD of the generated light and the target SPD is observed. In the tests performed, relative rms errors in the range of 1%–20% are achieved. The two main drawbacks of the system are the low intensity values in the short-wavelength region and the low contrast of the LCD panel. Both can be significantly improved by replacing the LCD panel with an upgraded model.

Combined with the new software, the spectral integrator has potential applications to a wide range of

Table 1. Relative Spectral rms Error^a for the SPD of the Generated Light Before and After Including the Spectral Integrator and the Spectroradiometer in the Optimization Loop

Stimulus	Before $e_{\text{rms,rel,pre}}$ (%)	After $e_{\text{rms,rel,post}}$ (%)
Illuminant A	1.40	0.57
Illuminant C	7.94	7.42
Illuminant D65	8.49	7.49
Illuminant E	12.99	11.99
Measured SPD of light source TL84	9.37	8.23
Measured SPD of light source Cool White Deluxe	11.02	10.73
Green optimal color	4.79	5.52
Magenta optimal color	25.18	24.54
SPD of the Stiles reference stimulus B, centered at 444.4 nm	20.76	19.76
SPD of the Stiles reference stimulus G, centered at 525.3 nm	5.65	3.03
SPD of the Stiles reference stimulus R, centered at 645.2 nm	27.38	29.57
Gaussian shaped SPD centered at 570 nm, with a 50 nm bandwidth	1.26	0.45
Gaussian shaped SPD centered at 500 nm, with a 20 nm bandwidth	3.12	1.09
Gaussian shaped SPD centered at 490 nm, with a 5 nm bandwidth	27.34	27.90
Bimodal SPD	0.93	0.18

^aThe errors are given in %.

fields, some of which will be investigated in the future. Particular projects of interest include investigation of the transformability of color-matching functions,^{15–18} metamerism,¹⁹ chromatic adaptation and color-appearance modeling,^{20–23} multispectral image acquisition,^{24,25} and spectral characterization of digital cameras.^{26,27}

References

- M. Hauta-Kasari, K. Miyazawa, S. Toyooka, and J. Parkkinen, "Spectral vision system for measuring color images," *J. Opt. Soc. Am. A* **16**, 2352–2362 (1999).
- M. Gasser, H. Bilger, H.-D. Hofmann, and K. Miescher, "Spektraler Farbintegrator," *Experientia* **15**, 52–53 (1959).
- P. Weisenhorn, "Der Spektrale Farbintegrator und seine Entwicklung," in *Proceedings of the International Color Conference* (Luzern, 1965), pp. 415–420.
- A. Valberg, *Spektraler Farbintegrator, Kompendium* (Universität Basel, 1966).
- I. Østby, "Konstruktion, Bau und Eichung eines Spektralintegrators für visuelle Farbenmessung," Master's thesis (University of Oslo, 1972).
- A. Valberg, T. Seim, and P. Sällström, "Colour rendering and the three-band fluorescent lamp," in *Proceedings of the 19th Session of the CIE* (Bureau Central de la CIE, Paris, 1979), pp. 218–223.
- H. H. Razavi, "Using liquid crystal display (LCD) to modulate the visual spectrum," Master's thesis (University of Oslo, 2000).
- T. Seim and H. H. Razavi, "Color generation through complete spectral control," in *Colour Between Art and Science, Proceedings of the Oslo International Colour Conference*, E. Wessel, ed. (Institute of Colour, Norwegian College of Arts and Design, Oslo, 1998), pp. 166–167.
- T. Søndrol, L. E. Hoel, T. Aspelund, and J. Skjerven, "Styringsprogram for spektralintegrator (Executive software for a spectral integrator)," B.S. thesis (Gjøvik University College, Norway, 2003).
- I. Farup, T. Seim, J. H. Wold, and J. Y. Hardeberg, "Generating stimuli of arbitrary spectral power distributions for vision and imaging research," in *Human Vision and Electronic Imaging IX*, Proc. SPIE **5292**, 69–79 (2004).
- C. Blum and A. Roli, "Metaheuristics in combinatorial optimization: overview and conceptual comparison," *ACM Comput. Surv.* **35**, 268–308 (2003).
- R. W. Floyd and L. Steinberg, "An adaptive algorithm for spatial grayscale," in *Proceedings of the Society for Information Display* (SID, San Jose, 1976), Vol. 17, pp. 75–77.
- W. S. Stiles and J. M. Burch, "Interim report to the Commission Internationale de l'Eclairage, Zurich, 1955, on the National Physical Laboratory's investigation of colour-matching (1955)," *Opt. Acta* **2**, 168–181 (1955).
- W. S. Stiles and J. M. Burch, "N.P.L. colour-matching investigation: final report (1958)," *Opt. Acta* **6**, 1–26 (1959).
- W. A. Thornton, "Toward a more accurate and extensible colorimetry, Part I: Introduction. The visual colorimeter-spectroradiometer. Experimental results," *Color Res. Appl.* **17**, 79–122 (1992).
- W. A. Thornton, "Toward a more accurate and extensible colorimetry, Part II: Discussion," *Color Res. Appl.* **17**, 162–186 (1992).
- W. A. Thornton, "Toward a more accurate and extensible colorimetry, Part III: Discussion (continued)," *Color Res. Appl.* **17**, 240–262 (1992).
- Commission Internationale de l'Eclairage, *Volunteer Labs Sought to Test Foundations of Colorimetry*, Activity Report for TC1-56 Improved Colour Matching Functions (CIE, 2001).
- G. Wyszecki and W. S. Stiles, *Color Science: Concepts and Methods, Quantitative Data and Formulae* (Wiley, 1982).
- M. D. Fairchild, *Color Appearance Models* (Addison-Wesley, 1997).
- J. von Kries, "Theoretische Studien über die Umstimmung des Sehorgans," in *Festschrift der Albrecht-Ludwigs-Universität in Freiburg zum fünfzigjährigen Regierungs-Jubiläum Seiner Königlichen Hoheit des Grossherzogs Friedrich* (C. A. Wagner's Universitäts-Buchdruckerei, Freiburg i. Br., 1902), pp. 143–158.
- C. Li, M. R. Luo, B. Rigg, and R. W. G. Hunt, "CMC 2000 chromatic adaptation transform: CMCCAT2000," *Color Res. Appl.* **27**, 49–58 (2002).
- N. Moroney, M. D. Fairchild, R. W. G. Hunt, C. Li, M. R. Luo, and T. Newman, "The CIECAM02 color appearance model," in *Proceedings of the Society for Imaging Science and Technology and the Society for Information Display's 10th Color Imaging Conference: Color Science and Engineering: Systems, Technologies, Applications* (IS&T, Springfield, 2002), pp. 23–27.
- J. Y. Hardeberg, *Acquisition and Reproduction of Color Images: Colorimetric and Multispectral Approaches* (dissertation.com, Parkland, Fla. 2001).
- J. Y. Hardeberg, F. Schmitt, and H. Brettel, "Multispectral color image capture using a liquid crystal tunable filter," *Opt. Eng.* **41**, 2532–2548 (2002).
- J. Y. Hardeberg, H. Brettel, and F. Schmitt, "Spectral characterization of electronic cameras," in *Electronic Imaging: Processing, Printing, and Publishing in Color*, Proc. SPIE **3409**, 100–109 (1998).
- H. Sugiura, T. Kuno, and H. Ikeda, "Methods of measurement for colour reproduction of digital cameras," in *Digital Solid State Cameras: Designs and Applications*, Proc. SPIE **3302**, 113–122 (1998).